High Resolution Diffusion Tensor Imaging of the Human Brain at 7T

Ralf Luetzkendorf[1], Sebastian Baecke[1], Johannes Mallow[1], Tim Herrmann[1], Joerg Stadler[3], Claus Tempelmann[2], Thomas Trantzschel[1], Johannes Bernarding[1]

[1]Institut für Biometrie und Medizinische Informatik, [2]Klinik für Neurologie, Medizinische Fakultät, Otto-von-Guericke-Universität, Leipziger Straße 44, 39120 Magdeburg. [3]Leibniz Institut für Neurobiologie, Brennecke Strasse 6, Magdeburg.

ralf.luetzkendorf@med.ovgu.de

Abstract: Magnetic resonance imaging (MRI) at 7T provides higher signal-to-noise ratio (SNR) which enables high-resolution functional and anatomic MRI. There is also an increased demand for high-resolution diffusion tensor imaging (DTI) providing important information about cell physiology and neuronal connectivity. DTI may also profit from higher SNR as diffusion-weighting reduces the signal exponentially. But the potential SNR gain in ultra-high field (UHF) DTI is counterbalanced mainly by shortened T_2 relaxation times of brain tissue, increased signal inhomogeneities, and coil parameter dependencies for parallel imaging. High resolution DTI (1.15/1.15/3.0 mm^3) was performed at 3T and 7T. Parallel imaging (GRAPPA, reconstruction factor 3) and data averaging was required to reduce image distortions, inhomogeneous signal distribution, and increase SNR. This allowed calculating high resolution Diffusion tensor and fractional anisotropy maps. In temporal and basal regions the reduced signal-to-noise ratio rendered the calculated parameter maps less reliable. A simulation of the distribution of the excitation radio frequency (RF) field at 7T in a human voxel model revealed that the inhomogeneities of brain tissue leads to inhomogeneous excitation which is a major cause for observed signal voids. High resolution DTI is therefore feasible at 7T with an image quality comparable or superior to 3T DTI. Main advantage for 7T DTI is combining DTI with anatomic and functional MRI acquired at 7T on the same MR scanner thereby reducing registration errors.

1 Introduction

Diffusion-weighted imaging and the extension to Diffusion tensor imaging (DTI) are standard techniques to detect pathological changes of water diffusion on a cellular scale such as caused by ischemic stroke [MCK90][WCL92][BBH00], or to track non-invasively the fiber tracts in the brain that connect different neuroanatomical regions [BBH00][BUS06]. However, compared to DTI at 1.5T rather few DTI studies were performed on higher magnetic field strengths [SHT03][JCP04][HPD10] [MHX08][RVW12]. In principle, the increased signal-to-noise ratio (SNR) provided by ultra-high fields (UHF) such as 7 T or higher should be advantageous to increase spatial resolution or to apply stronger diffusion-weighting, as both reduce considerably the SNR. This strategy could help to resolve multi-exponential diffusion behaviour in different physiologic compartments [BUS06], to detect very small pathologies, or to

analyze crossing neuronal fibers in more detail. However, UHF conditions impose new severe problems such as increased susceptibility artefacts, reduced T_2* time, increased specific absorption rate (SAR), increased inhomogeneity of the applied excitation radio frequency (RF) field, and decreased T_2 relaxation times of brain tissue [HAF12] [MRX08] [RVW12]. In particular, the shortened T_2 times and the RF field inhomogeneities are the main obstacles for a straightforward implementation of DTI at UHF which will be discussed in more detail below. Although it was argued that DTI at 7T provides no real advantages to 3T DTI [SZ09] considering the much more costly and technically demanding hard- and software new studies analysed the complex inter-dependencies between different image acquisition parameters [MHX08][RVW12]. The main advantage of DTI at 7T would be the simultaneous measurement of high resolution anatomic and functional MRI (fMRI) together with high resolution DTI as this could enable to minimize registration errors resulting from performing measurements of the same person on different scanners. Therefore, it should be considered already as a progress if image and data quality at 7T DTI would be comparable to 3T DTI since this would allow to ameliorating the integration of anatomic, functional, and microstructural information.

To acquire acceptable high resolution DTI at ultra-high fields is difficult due to technical and biophysical restrictions: Single shot EPI is as usually used for DTI is sensitive to susceptibility variations within the probe volume. The susceptibility artefacts increase with the strength of the polarizing magnetic field (B_0-field). Increasing the matrix size prolongs the echo-train length which, due to the stronger field-dependent T_2^*-decay and off-resonance effects will lead to additional image blurring. When inserting diffusion-weighting gradients into the pulse sequence, echo time (TE) is prolonged even more. As T_2 relaxation times of brain tissue shorten with increasing B_0, T_2-decay-related effects will lead to very small SNR especially when applying strong diffusion-weighting. However, combining parallel imaging techniques with partial Fourier imaging enables the acquisition of high resolution DTI at 3T and 7T [JCP04][RVW12]. The increased B_0 leads to additional challenges. At 7T or higher the RF wavelength within biological tissue gets comparable to the dimensions of the examined object. Resulting interference effects lead to inhomogeneous distribution of the RF flip angle within the volume-of-interest which may cause substantial signal losses [TCB06]. Specially designed measurement sequences such as segmented-readout sequences [HPD10] or special hardware such as phased-array coils with more elements can reduce image distortions but they still suffer from some restrictions such reduced volumes of interest or prolonged examination time. As experimental sequences may also not be generally available to all users the study aimed to investigate whether in vivo DTI of the human brain would be feasible at 7T using standard equipment and a vendor-provided double spin echo DTI sequence (used to reduce eddy current artefacts). For comparison, DTI at 3T was performed using a similar protocol.

To gain more insight the inhomogeneous RF distribution the RF field of an 8 element phased-array coil was simulated and the according signal loss due to deviations from the nominal flip angle were used to estimate the resulting signal losses if using the double-spin echo DTI sequence provided by the vendor.

2 Material and Methods

2.1 Image acquisition

Six healthy volunteers were examined after giving written consent according to the local ethics committee of the University Clinic Magdeburg according to the declaration of Helsinki. DTI was performed on a 3T whole body scanner (Trio, SIEMENS, Germany, Syngo VA25A), maximum gradient strength 40mT/m, 8 element phased-array (PA) head coil (Siemens), and a 7T whole body scanner (SIEMENS, Syngo VB12T), maximum gradient strength 38mT/m, 8-element PA head coil (Rapid, Wurzburg, Germany). Each volunteer was examined at 3T before being scanned at 7T. Diffusion-weighting was carried out with 6 directions ([+X,-Z];[-X,-Z];[-Y,-Z];[-Y,+Z];[+X,-Y];[-X,-Y]), or 12 directions ([+X,-0.5Z];[-0.5Y,-Z];[0,5X,-Y];[X,-0.5Y];[-Y,-0.5Z];[0.5X,-Z];[+X,0.5Z]; [0.5Y,-Z];[-X,-Y];[X,0.5Y];[-Y,0.5X];[-0.5X,-Z]), maximum b-value was 3000 s/mm^2. Image parameters were 6/8 partial-Fourier, matrix size 192^2 (1.15 mm x 1.15 mm), slice thickness 3 mm, slice distance 10%, field-of-view (FoV) 220 mm, TR = 10 s (3T) resp. 9s (7T), TE = 83 ms (3T) resp. 80 ms (7T). TE was set near to the minimal values of the according sequence parameters. GRAPPA was used for reconstruction.

2.2 Data postprocessing

Averaging on the MR scanner led to blurring of the image due to an in-plane inter-scan shift between subsequent runs that was not corrected by the vendor-provided sequence. Therefore, all runs had to be acquired as single data sets, and subsequently transferred to an external computer for averaging. In the first step, the images with and without diffusion-weighting were registered separately for each diffusion-weighting direction using a home-built program based on a cross-correlation algorithm implemented in Matlab (xcorr2, Matlab2008, www.mathworks.com). The cross-correlation was calculated by convolving two images and determining the x- and y-shifts where the convolution exhibited a maximum. Images were accordingly shifted and subsequently averaged. Usually, averaging of 4 up to 8 data sets was required for an acceptable image quality. The image quality was determined visually as a reliable quantitative determination of the signal-to-noise ratio (SNR) in multi-channel coil imaging requires special time-consuming measurement protocols which were beyond the duration of our study [DRR08]. The open source software FSL (version 4.1, http://www.fmrib.ox.ac.uk/fsl/) was used for calculation of the maps of isotropic apparent diffusion coefficients (ADC), and determination of the principal diffusion directions (PDD). The calculations included extraction of the brain tissue, eddy current correction, and Bayesian estimation of diffusion tensors. No additional post-processing such as smoothing or distortion correction was applied.

2.1 Simulation and analysis of the B_1 inhomogeneity

To estimate how an inhomogeneous the distribution of the radio frequency (RF) excitation may cause signal losses we simulated an 8-element phased-array coil and the

according RF field using a commercial software (CST MICROWAVE STUDIO 2009, http://www.cst.com) [MHC11]. To analyze general effects of inhomogeneously distributed biological tissue on the B_1 field independent of the examined volunteers, a software model of a human head was included into the simulation (HUGO, CST MICROWAVE STUDIO 2009).
Inhomogeneities in the RF field correspond to deviations from the nominal flip angle. The deviations are further amplified by the double-spin echo sequence which underlies the vendor-provided DTI sequence used in this study: the second spin echo S_{21} at TE_2 within a double spin echo sequence (θ_1 - θ_2 - θ_2) can be calculated to

$$S_{21} = M_{SS} \sin(\theta_1) \sin^4\left(\frac{\theta_2}{2}\right) \exp\left(-\frac{TE_2}{T_2}\right), \quad [1]$$

where M_{ss} is the steady-state magnetization [HBV99][BKZ04] [RJL07]

$$M_{SS}(TR, T_1, \theta_1, \theta_2) = M_0 \frac{1 + (\cos(\theta_2) - 1)\cos(\theta_2)E_4 + (1 - E_5) - \cos^2(\theta_2)E_3}{1 - \cos(\theta_1)\cos^2(\theta_2)E_3}, \quad [2]$$

and

$$E_3 := \exp\left(-\frac{TR}{T_1}\right), \quad E_4 := \exp\left(-\frac{TE_2}{2T_1}\right), \quad E_5 := \exp\left(-\frac{TR - (TE_1 + TE_2)/2}{T_1}\right). \quad [3]$$

The amplification of a deviation from the nominal flip angle can be estimated by inserting the parameters of the DTI measurement (TE_1 = 35 ms, TE_2 = 85 ms, TR = 9 s, and θ_2=2θ_1) and relaxation times at 7T with T_1 = 2130 ms (gray matter), T_1 = 1220 ms (white matter), T_1 = 4400 ms (cerebrospinal fluid), and T_2 = 59 ms (gray matter), T_2 = 54 ms (white matter), T_2 = 2000 ms (cerebrospinal fluid) according to [RJL07].

3 Results

The simulation shows that the excitation is quite homogeneous in the central part of the volume of the coil (fig. 1a). Introducing the commercial voxel model HUGO with dielectric properties similar to those of human brain tissue changes the magnetic part of the RF excitation field (proportional to the B_1 field) grossly. This is due to the shortened wavelength within biological tissue and the inhomogeneous distribution of the biological tissue within the skull exhibiting compartments filled with gray matter, white matter, blood, and cerebrospinal fluid. In the simulation, local reductions of the B_1 field down to about 50% of the surrounding parts can be seen (fig. 1 b). Similar effects can be seen on the in-vivo measurements (fig. 1d,e). Especially on the diffusion-weighted image (fig. 1e) the temporal and frontal parts are prone to signal losses or distortions.

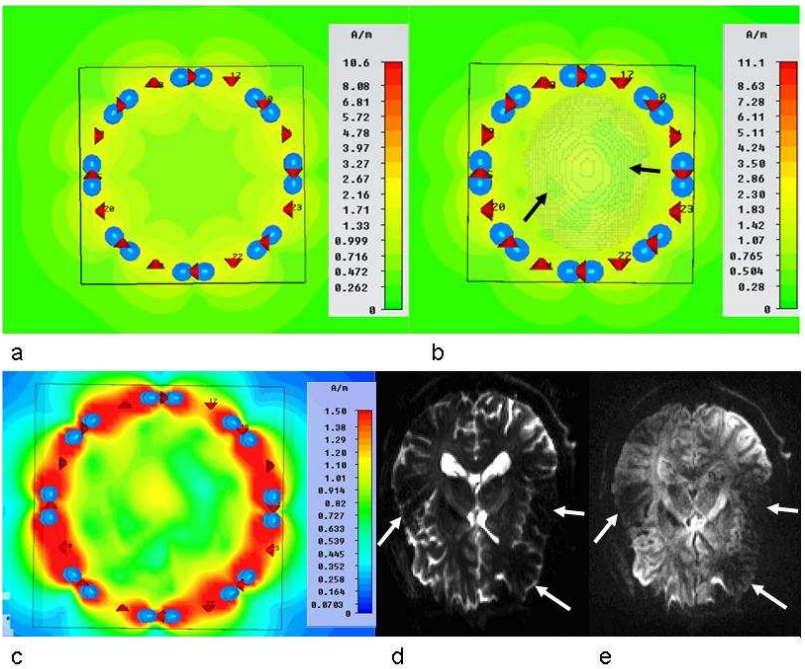

Figure 1: Simulation of an 8-element phased-array coil, the according distribution of the electromagnetic excitation field, and the influence of a biological load on the excitation field. (a-c) One representative slice of the magnetic part of the excitation field generated by an 8-element phased-array transmit/receive coil. The colors encode logarithmically for the field strength. (a) field distribution without load. (b) Inserting the head of the HUGO Human Body Model (model depicted by light-gray lines) leads to an inhomogeneous distribution for the excitation field with local signal reductions of up to 45% relative to the surrounding areas (black arrows). (c) For better visualization the color encoding of (b) was contrast-optimized and the overlay of the HUGO software model was removed. (d, e) Representative slice of a T_2-weighted double-spin echo image without (d) and with diffusion weighting (e); local signal reductions (arrows) are further amplified by diffusion-weighting leading to strong signal losses.

The major improvement of the image quality was achieved by applying parallel imaging. A GRAPPA factor of 2 reduced TE to about 95 ms while GRAPPA 3 led to a TE of about 85 ms. This in turn reduced the echo train length and thereby the EPI-related distortion artefacts. At GRAPPA 4 the image quality deteriorated again due to increased noise. As diffusion-weighting increases TE additional SNR loss the fore-mentioned effects were even more critical. Interestingly in part of the examinations, we observed local signal voids (fig. 1d, 1e) even when applying parallel imaging with GRAPPA 2 or 3. These signal variations seemed to depend partly on the individual anatomy, coil filling, or precise position of the head in the coil. The main cause for the signal variations were probably B_1 inhomogeneities. This is supported by the simulation of the RF field under load conditions (fig. 1b, 1c) as well as the calculation how these deviations from the actual flip angle of the excitation RF field were amplified by the

double spin echo sequence. According to eq. 1-3, a drop of the actual flip angle to 50% of the nominal flip angle will lead to a reduction of the nominal signal (S_{21}) to about 20%. This initial signal drop is reduced further after turning on diffusion-weighting which decreases the signal exponentially. Regions with reduced initial signal may therefore exhibit almost no signal in DTI (fig. 1e) leading to unreliable calculations of parameters such as apparent diffusion coefficients (ADC) or diffusion tensors.

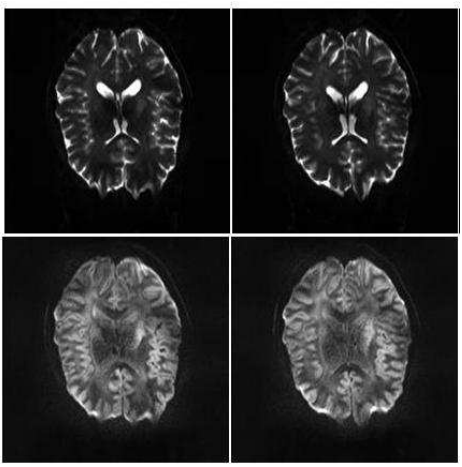

Figure 2: DTI with optimized parameters at 7T (GRAPPA 3, average of 8 data sets. Upper row: no diffusion weighting; lower row: diffusion weighted images, b=800 s/mm^2). Two out of twelve consecutive axial slices are displayed. The frontal sinus cause increasing distortions in the cranial images.

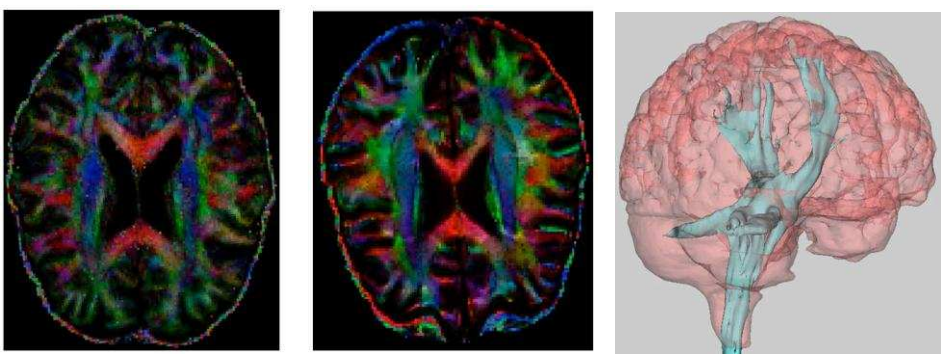

Figure 3: Color-encoded maps of the principal diffusion tensor direction (PDD maps) at 3T (left) and 7T (middle), calculated from two images (b-factor 0 and 800 s/mm², 12 directions as described in methods**,** GRAPPA factor 3). Red, green, and blue encode for the diffusion in (x, y, z)-direction according to the description in (http://www.fmrib.ox.ac.uk/fsl/fslview/dti.html). The noise in main fiber tracts such as corpus callosum is less at 7T then at 3T. The right image shows the reconstructed motor pathway (light blue) using 7T DTI data overlaid on brain (light red).

With the available standard equipment and the vendor-provided double-echo sequence a value of b = 800 s/mm^2 led to the best compromise between diffusion-weighting required for calculation of the ADC-values, and acceptable SNR. Higher b-factors increased TE and led to additional signal losses. We found that a matrix size of 192^2 and averaging 4 to 8 data sets represented a good compromise between the time required for data acquisition and increase of SNR in regions with signal drops (fig. 2). For comparison maps of the principal diffusion tensor direction (PDD maps) of a representative volunteer are shown in fig. 3.

4 Discussion and conclusion

The simulation of the electromagnetic fields showed that signal voids are due to a complex interaction between different parameters govering UHF MRI. (1) While in air the Larmor frequency of 297 MHz (7T) leads to a wavelength of approximately 1 m this wave length is considerably shortened in biological tissue due to the increase of the dielectric constant in water (vacuum: ε_r = 1.0, water: ε_r = 80). This may lead to interferences and standing wave effects with concomitant signal voids. (2) Deviations from the nominal flip angle are also amplified since diffusion-weighting requires refocusing pulses. Reducing eddy-current effects by applying double-refocused spin echo sequences may amplify strongly the applied RF field. For a single loop element this was analyzed in great detail [RVW12] and it was shown that the different parameters depend strongly from each other. (3) Applying advanced techniques such as q-ball imaging requires shortening of TE as T_2-values of brain tissue are shorter at 7T than at 3T. It may be speculated whether segmenting the individual anatomy allowing to generate an individual voxel model may help to correct for the observed signal losses in the temporal and basal brain regions. However, as this was not yet realized in our project a potential increase in image quality using this strategy remains open for future projects.

Concerning the measurement protocol, the largest improvement will result by reducing the inherent B_1 inhomogeneity and shortening the echo time. As the probe volumes are in the order of the excitation RF wavelength under load conditions, flip angles within the object are ill-defined which in turn can cause significant signal losses amplified by the inherent SNR reduction due to diffusion-weighting (fig.1d,e). Additionally, the signal voids seemed to depend on the individual anatomy, coil filling and precise position of the head in the coil. A similar observation was made by Truong et al. [TCB06] who provided a thorough analysis how the different factors influence signal behaviour in ultra-high field MRI. At 8T large deviations between nominal flip angles of 90°/180° were measured leading to real flip angles ranging from 102°/214° to 47°/94°. Accordingly, substantial local signal losses were detected already for single echo spin echo sequences [TCB06]. This effect is even more amplified in double spin echo sequences such as in the underlying vendor-provided DTI sequence of our project. It may therefore be concluded that observed signal losses are mainly due to locally reduced excitation energies that are additionally amplified by the double spin echo and the shortened T_2 relaxation times at ultra-high field conditions.

This shortening of the T_2 relaxation times is the second main restriction of DTI at ultra-high field. Both insertion of refocusing pulses for eddy current correction and applying diffusion gradients prolong considerably the echo time, especially in the applied double spin echo sequence, leading to severe signal losses. Therefore, the main strategy to improve DTI at ultra-high fields consists in shortening echo time by applying diffusion-weighting sequences with a single refocusing pulse [Fi09], increasing gradient power to shorten diffusion gradient durations, or using phased-array coils with more coil elements [LBS09]. However, these strategies impose severe technical and costly needs on the hardware. The inherent SNR loss due to increasing the GRAPPA factor may be counterbalanced by the increased SNR provided by the higher field strengths, or by applying more directions of the diffusion-encoding gradients although the latter strategy prolongs total examination time considerably.

The increased physiological noise at higher field strengths [HJS11] imposes also restrictions on the SNR gain at 7T but figure 3 demonstrates that a reliable determination of the principal directions of the diffusion tensor is feasible in good quality at 7T. Recently, segmented EPI showed very promising results for DTI at 7T but at the expense of longer acquisition times and smaller volume [HPD10]. To what extend the image quality can be increased by the use of phased-array coils with more elements and applying single echo DTI sequences as well as higher gradients has also to be analyzed in future experiments. Additional sequence optimization such as segmented read-out techniques [HPD10], optimized pulses, or reducing TE by applying diffusion-weighted sequences with a single refocusing pulse [Fi09] may also improve image quality. Stronger diffusion encoding gradients will also be advantageous as this allows shortening the gradient duration. It is therefore to be expected that DTI at 7T and higher can be improved significantly to fully exploit the advantages of ultra-high fields.

One may question whether the results merit the considerably higher technical efforts of DTI at ultra-high field MRI. The answer is clearly positive. The study (fig. 3) demonstrated that single-shot EPI-based DTI at 7T using standard 8-channel phased-array coils and the vendor-provided double-spin echo DTI sequence led to diffusion-weighted images with good quality. However, parallel imaging is indispensable to reduce susceptibility artefacts and distortions both at 3T and 7T [JCP04][HPD10], and parallel imaging factors between 2 and 3 are best suited to strongly reduce EPI-related artefacts while still preserving a good SNR. The SNR was better in 7T DTI than in 3T except for some frontal, temporal and basal brain regions.The main fiber tracts such as the corpus callosum showed most impressively the advantage of 7T over 3T (fig. 3) which was also found by other studies [MHX08]. Additionally, even reaching the same image quality at 7T as in lower B_0 fields will already be advantageous: combining high-resolution DTI with complementary information such as high-resolution functional or anatomic imaging on the same MR scanner [BUS06][MSZ08][BUS06] will profit from the fact that data acquired at the same scanner in the same session will greatly reduce registration errors. This allows taking advantage of the inherent higher SNR at 7T to increase the resolution, and therefore to gain more details about anatomic, functional, and physiologic mechanisms such as functional connectivity except for the above mentioned brain regions with increased distortion effects.

We want to thank Dr. Juergen Braun for the helpful discussions.

We acknowledge a grant of the German Research Foundation (DFG, Be 1824/8-1).

References

[BBH00] Bernarding, J.; Braun, J.; Hohmann, J.; Mansmann, U.; Hoehn-Berlage, M.; Stapf, C. Et al.: Histogram-based characterization of healthy and ischemic brain tissues using multiparametric MR imaging including apparent diffusion coefficient maps and relaxometry. In: Magn Reson Med 43, 2000; S. 52–61.

[Bi03] Le Bihan, D.: Looking into the functional architecture of the brain with diffusion MRI. In: Nat. Rev. Neurosci 4 (6), 2003; S. 469–480.

[BKZ04] Bernstein M.A.; King, F.K.; Zhou X.J. (Hg.): Handbook of MRI Pulse Sequences: Elsevier Academic Press, 2004.

[BPP00] Basser, P. J.; Pajevic, S.; Pierpaoli, C.; Duda, J.; Aldroubi, A.: In vivo fiber tractography using DT-MRI data. In: Magn Reson Med 44 (4), 2000; S. 625–632.

[BUS06] Le Bihan, D.; Urayama, S.; Aso, T.; Hanakawa, T.; Fukuyama, H.: Direct and fast detection of neuronal activation in the human brain with diffusion MRI. In: Proc. Natl. Acad. Sci. U.S.A 103 (21), 2006;S. 8263–8268.

[Fi09] Finsterbusch, J.: Eddy-current compensated diffusion weighting with a single refocusing RF pulse. In: Magn Reson Med 61 (3), 2009; S. 748–754.

[GSB07] Gilbert, G.; Simard, D.; Beaudoin, G.: Diffusion Tensor MRI: Combination of Signals from Phased Array Coils. In: Proceedings of the joint annual meeting of the ISMRM-ESMRMB, Berlin, 2007; S. 6.

[HAF12] Heidemann R.M.; Anwander A.; Feiweier T.; Knösche T.R.; Turner R.: K-space and qspace: combining ultra-high spatial and angular resolution in diffusion imaging using ZOOPA at 7T; Neuroimage 60(2), Epub 2012 Jan9. PMID:22245337, 2012; S. 967-978.

[HBV99] Haacke, E.M.; Brown, R.W.; Thompson, V.R.: Magnetic Resonance Imaging: Physical Principles and Sequence Design: Wiley & Sons, 1999.

[HJS11] Hutton, C.; Josephs, O.; Stadler, J.; Featherstone, E.; Reid, A.; Speck, O. et al.: Theimpact of physiological noise correction on fMRI at 7 T. In: Neuroimage 57 (1), 2011; S. 101–112.

[HPD10] Heidemann, R.M.; Porter, D.A.; Anwander, A.; Feiweier, T.; Heberlein, K.; Knösche,T.R.; Turner, R.: Diffusion imaging in humans at 7T using readout-segmented EPI and GRAPPA. In: Magn Reson Med 64 (1), 2010; S. 9–14.

[HSK09] Hoffmann, M.; Stadler, J.; Kanowski, M.; Speck, O.: Retinotopic mapping of the human visual cortex at a magnetic field strength of 7T. In: Clin Neurophysiol 120 (1), 2009; S. 108–116.

[JCP04] Jaermann, T.; Crelier, G.; Pruessmann, K. P.; Golay, X.; Netsch, T.; van Muiswinkel, A. M. C. et al.: SENSE-DTI at 3 T. In: Magn Reson Med 51 (2), 2004; S. 230–236.

[LBS09] Luetzkendorf, R.; Baecke, S.; Stadler, J.; Tempelmann, C.; Bernarding, J.: Diffusion weighted imaging at 3T and 7T: comparison of different phased array head coils. In: 15th annual meeting of the organization for Human brain Mapping, San Francisco, 2009; S. F 275 AM4.